THE JOURNAL OF PHYSICAL CHEMISTRY B LETTERS

2006, *110,* 19100−19103
Published on Web 09/07/2006

Catalyzed Radical Polymerization of Styrene Vapor on Nanoparticle Surfaces and the Incorporation of Metal and Metal Oxide Nanoparticles within Polystyrene Polymers

Victor Abdelsayed, Edreese Alsharaeh, and M. Samy El-Shall*

Department of Chemistry, Virginia Commonwealth University, Richmond, Virginia 23284-2006

Received: July 24, 2006; In Final Form: August 16, 2006

We present a novel approach to polymerize olefin vapors on the surfaces of metallic and semiconductor nanoparticles. In this approach, a free radical initiator such as AIBN is dissolved in a volatile solvent such as acetone. Selected nanoparticles (prepared separately using the laser vaporization-controlled condensation method) are used to form initiator-coated nanoparticles placed on a glass substrate. The olefin (styrene) vapor is polymerized by the thermally activated initiator on the nanoparticle surfaces. Our approach also provides structural and mechanistic information on the early stages of catalyzed gas-phase polymerization, which can be used to correlate the gas-phase structural properties with the bulk properties and the performance of the polymer nanocomposites. This correlation is the key step in controlling the properties of the polymer nanocomposites. Our results clearly demonstrate the success of this method in preparing polymer coated nanoparticles for a variety of interesting applications. The precise control of the chemical functionality, thickness, and morphology of the polymer film and the size, size distribution, and properties of the core nanoparticles (photoluminescence, magnetic) may lead to major technological breakthroughs in a variety of applications including drug delivery, ultrasensitive detectors, and chemical and biological sensors.

The development of new methods to synthesize novel hybrid materials that combine several properties such as strength, toughness, lightweight, elasticity, electrical conductivity, and improved electrooptic performance is crucial for scientific and technological advances. Recently, metal nanoparticles embedded in host polymer matrixes have become the focus of increasing attention because the properties of these materials can be tailored by altering the metal particles, their size and shape distributions, or their relative concentrations.[1−9]

Polystyrene is among the most important polymers that is commonly used in a variety of products ranging from home insulation products and drinking cups to plastic cutlery and a variety of other applications. Gas-phase self-initiated and catalyzed polymerizations of styrene have been investigated using a vapor phase nucleation approach.[11−13] In this approach, supersaturated styrene vapor is doped with a small amount of a free radical initiator such as peroxides. The growing polymers in the vapor phase act as "condensation nuclei" for the formation of observable liquid drops (presumably containing styrene oligomers and monomers), which can be detected by light scattering.[11−13] Because of the ultrasensitivity of the nucleation phenomena, one can, in principle, detect a single polymer molecule (oligomer) from the vapor phase.[13] Unfortunately, the nucleation approach provides only speculation on the polymer formation in the vapor phase because it detects the consequence of the polymerization process and it is not possible to isolate the polymer molecules, characterize their structures, or measure their physical properties. Although metal nanoparticles can provide efficient condensation centers for the growing polymers in the gas phase, the incorporation of metal nanoparticles within polystyrene polymers formed by gas-phase polymerization has not been reported. In this letter, we present a new approach for the catalyzed radical polymerization of styrene vapor on the surfaces of metal and metal oxide nanoparticles. Furthermore, we provide direct evidence for the catalyzed radical-initiated polymerization of styrene in the gas phase and obtain structural information on the styrene dimer formed by the reaction of styrene vapor with a free radical initiator.

The general approach utilized in the present work involves polymerization of olefin vapors on the surfaces of metallic, semiconductor, or metal oxide nanoparticles. In this approach (see Figure 1), a free radical initiator such as 2,2′-azobisisobutyronitrile (AIBN) is dissolved in a volatile solvent such as acetone. Selected nanoparticles, prepared separately using the laser vaporization-controlled condensation (LVCC) method,[14] are sonicated in the initiator solution for an appropriate time. The solution is placed on a glass substrate where the solvent is gently evaporated. This process results in the formation of initiator-coated nanoparticles as well as initiator-coated substrate surfaces where no nanoparticles are present. The substrate is then heated (90 °C) inside a vacuum chamber where an olefin vapor is admitted at a controlled flow rate. The olefin vapor is then polymerized by the activated initiator on the nanoparticle surfaces as well as on the glass substrate, and the resulting polymers encapsulate the nanoparticles by forming a polymer coating on the surface. It is clear that this approach results in polymer formation on the nanoparticle surfaces as well as on the substrate surfaces. However, by controlling the concentration of the nanoparticles in the initiator solution, it is possible to control the density of the deposited nanoparticles on the substrate

* Corresponding author. E-mail: selshall@hsc.vcu.edu.

10.1021/jp064720p CCC: $33.50

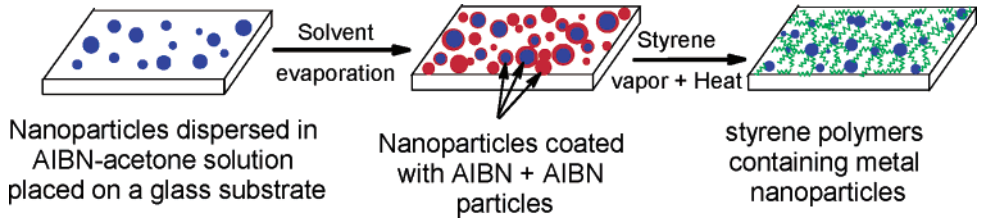

Figure 1. Illustration of the method used to polymerize styrene vapor on the activated nanoparticle and substrate surfaces.

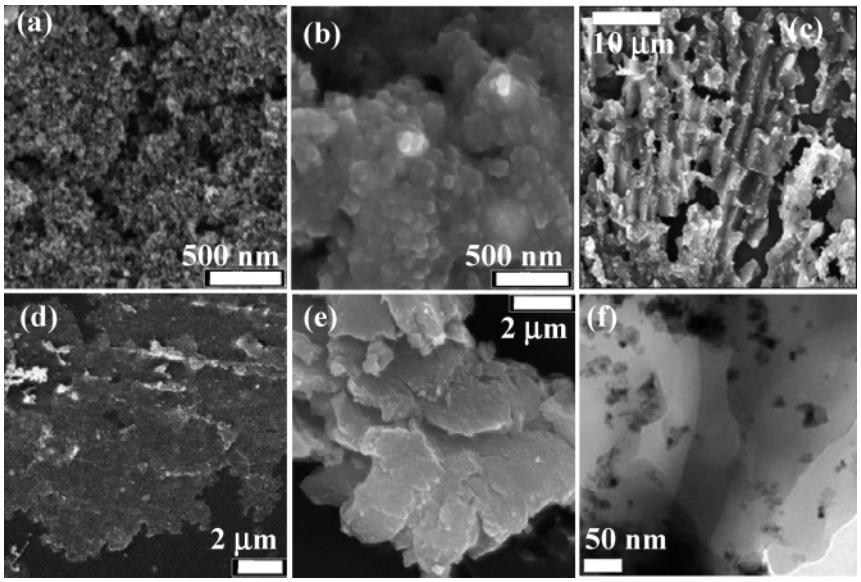

Figure 2. SEM micrographs of Ni nanoparticles deposited on a glass substrate (a) before and (b) after the exposure to thermally heated styrene vapor. (c) SEM of polystyrene formed on Ni nanoparticles coated with AIBN. SEM micrographs of Fe_2O_3 nanoparticles coated with AIBN (d) before and (e) after the exposure to heated styrene vapor. (f) TEM image of polystyrene coated Fe_2O_3 nanoparticles.

surface and, consequently, the relative amount of polymer-containing nanoparticles.

Several techniques have been used to characterize the nanoparticle polystyrene composites formed using the current approach. The morphology of the composites appears to change with the nature of the nanoparticles and the concentration of the initiator. Parts a and b of Figure 2 display SEM images of the Ni nanoparticles deposited on a glass substrate before and after the exposure to heated styrene vapor, respectively. It is clear that the self-initiated thermal polymerization of styrene vapor results in the formation of thick polymer coatings on the aggregated nanoparticle surfaces, as shown in Figure 2b. However, in the presence of the AIBN initiator on the nanoparticle surfaces, polymerization of styrene vapor results in the formation of a rough texture deposit, as shown in Figure 2c. It is interesting that in the case of the Fe_2O_3 nanoparticles coated with AIBN (Figure 2d), a more smooth platelike deposit is formed upon the exposure of the coated nanoparticles to the heated styrene vapor, as shown in Figure 2e. The TEM images of the polymer-containing nanoparticles display the dispersive nature of the nanoparticles embedded in the polystyrene matrix, where nanoparticles with an average size less than 50 nm are randomly distributed in the polymer matrix with some agglomeration, as shown in Figure 2f.

The ^{1}H NMR spectrum of the polymer-containing Ni nanoparticles, displayed in Figure 3(a), shows no peaks in the 5−6 ppm region, indicating the absence of styrene monomer. The two sets of peaks observed at chemical shifts between 6 and 7 ppm and 1−2 ppm were assigned to the aromatic protons of polystyrene rings and to the protons of the sp^3 carbons in the aliphatic portion of polystyrene, respectively. The FTIR spectrum showed absorption features between 2850 and 2950 cm^{-1},

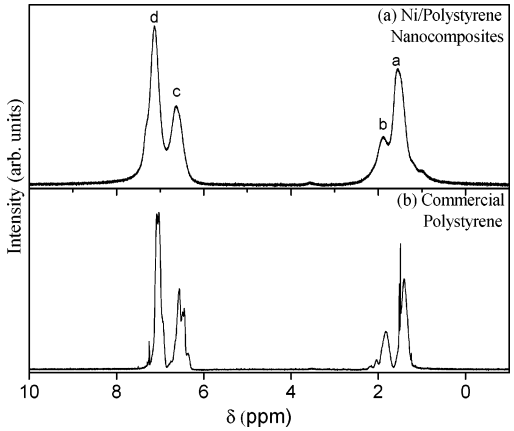

Figure 3. Comparison between the ^{1}H NMR spectra of (a) the prepared polystyrene containing Ni nanoparticles and (b) commercial polystyrene (Aldrich, 50 000 amu).

corresponding to the stretching vibrations of the C−H bond (sp^3 hybridization), which confirmed the opening of the vinyl group in the styrene monomer and the formation of polystyrene. Both the ^{1}H NMR and the FTIR spectra of the polystyrene formed on the Ni nanoparticles are nearly similar to those of commercial polystyrene (Supporting Information S1). The average molecular weight was determined by GPC analysis as 76 000 amu with polydispersity of 3.2. The glass transition temperature (T_g) for Ni−polystyrene composite was measured as 100.6 °C, slightly higher than that of the pure polystyrene (T_g = 100 °C).

The metal components in the nanocomposites were examined by X-ray diffraction (XRD) analysis. The XRD pattern of the Ni−polystyrene composite (Supporting Information S2) showed

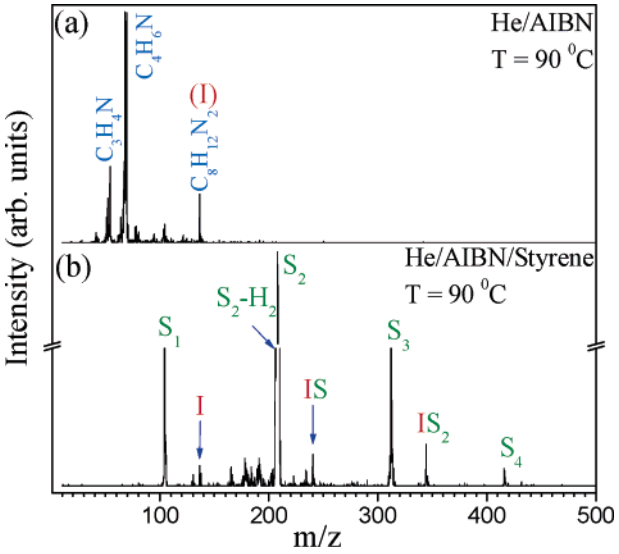

Figure 4. EI mass spectra obtained after heating AIBN in helium at 90 °C in the (a) absence and (b) presence of styrene vapor, respectively.

an amorphous pattern with weak broad peaks at (2θ) of 44.44° and 51.56°, assigned to the (111) and (200) planes, respectively, of the fcc crystal lattice of Ni. This result confirms that crystalline Ni particles were embedded in the amorphous polystyrene matrix.

To investigate whether the AIBN-catalyzed polymerization of styrene takes place in the gas phase, we used EI mass spectrometry to analyze the styrene vapor (in a He carrier gas) after flowing over an AIBN sample heated to 90 °C. Parts a and b of Figure 4 display the EI mass spectra of the AIBN obtained at 90 °C in the absence and presence of styrene vapor, respectively. In the absence of styrene, the major fragment ions observed of AIBN are $C_8H_{12}N_2^+$ (resulting from ionization of $C_8H_{12}N_2$ formed by the thermal decomposition of AIBN via a loss of N_2), $C_4H_6N^+$ (resulting from ionization of the C_4H_6N radical), and $C_3H_4N^+$. In the presence of styrene vapor, intense ion signals corresponding to ionized styrene oligomers (up to the tetramer) are observed, as shown in Figure 4b. In addition, small ion intensities resulting from the EI ionization of IS_n species, where I = $C_8H_{12}N_2$, S = styrene, and n =1, 2 are also observed. The styrene oligomers could have been formed by the thermal self-initiated (uncatalyzed) polymerization of styrene vapor.[15] However, EI ionization of styrene vapor heated to 90 °C in the absence of the AIBN initiator resulted in a very small ion intensity corresponding to the styrene dimer with the higher oligomers essentially absent. This indicates that the observed styrene oligomers in the presence of AIBN are most likely formed by a terminative process of the growing IS_n radicals, which results in the loss of (I) from the terminated oligomers. Thus, the mass spectrometry results confirm the AIBN-catalyzed polymerization of styrene vapor at 90 °C. On the basis of these results, we propose that the initiation and the early stages of styrene polymerization in the current experiments occur in the gas phase through the reactions with the heated ABIN molecules. The growing oligomers condense out of the gas phase on the surfaces of the nanoparticles and the glass substrate where chain propagation continues on the active radical sites. The net result is the formation of high-molecular-weight polymer chains that trap the nanoparticles and cover the substrate sites containing active radicals.

To obtain structural information on the styrene dimer formed through the gas-phase polymerization initiated by AIBN, we measured the collision cross-section (Ω) of the ionized dimer

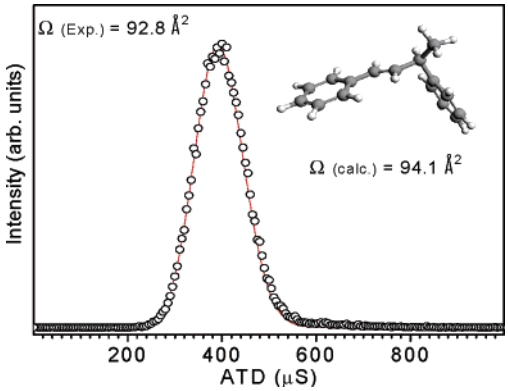

Figure 5. ATD of the ionized styrene dimer formed by AIBN initiation of styrene vapor.

using the ion mobility technique.[16−18] The mobility measurements can provide structural information on the ionized oligomers on the basis of their Ωs, which depend on the geometric shapes of the ions.[16−18] Theoretical calculations of possible structural candidates of the styrene dimer ions are then used to compute angle-averaged Ωs (using the trajectory method)[19] for comparison with the measured one. The agreement between the measured and calculated Ωs of candidate structures provides a reliable assignment of the structure of the dimer ions.

The ion mobility experiments were performed using the VCU mass-selected drift tube system, as described previously.[15,18] In these experiments, helium was used as a collision gas in a drift cell operating at a pressure of 1.7 Torr and a temperature of 29 °C under a uniform electric field of 1.5−3 V/cm.[15,18] Styrene dimer ions exiting the cell were mass-analyzed and collected as a function of time, yielding the arrival time distribution (ATD), shown in Figure 5, from which an Ω of 92.8 Å^2 was determined. It is important to note that no multiple peaks were observed in the ATD, indicating that only one dimer structure is present, as suggested by the excellent fit of the measured ATD to the calculated arrival time obtained from transport theory, as shown in Figure 5. The DFT B3LYP/6-31G** optimized structure[20] of the ionized styrene dimer (S_2) formed by the terminated radical initiation (shown in the inset of Figure 5) results in an average Ω of 94.1 Å^2 at 303 K, in excellent agreement with the measured Ω of S_2. It should be noted that, in the thermal self-initiated polymerization of styrene[15] (in the absence of a radical initiator such as AIBN), multiple dimer structures were identified (including the structure shown in Figure 5) and the broad ATDs could not be assigned to a single structure.[15] This indicates that the AIBN-catalyzed gas-phase polymerization of styrene results in one dominant structure of the dimer rather than a mixture of several different structures as in the spontaneous self-initiated polymerization where Diels−Alder adducts constitute the major products.[15,21]

In conclusion, we report a new method to incorporate metal, metal oxide, or semiconductor nanoparticles within polymers formed by free radical initiation of olefin vapors on the surfaces of activated nanoparticles. Our current goal is to explore the capabilities of this method in preparing different polymers and copolymers from olefin vapors on the surfaces of selected nanoparticles, nanorods, and nanowires characterized by unique electronic, photoluminescence, and magnetic properties. Our approach also provides structural and mechanistic information on the early stages of catalyzed gas-phase polymerization, which can be used to correlate the gas-phase structural properties with the bulk properties and performance of the polymer nanocomposites. This correlation is the key step in controlling the properties of the polymer nanocomposites.

Acknowledgment. We thank the National Science Foundation (CHE-0414613) for support of this work.

Supporting Information Available: FT-IR and XRD data of the polystyrene-containing metal nanoparticles. This material is available free of charge via the Internet at http://pubs.acs.org.

References and Notes

(1) Golden, J. H.; Deng, H.; DiSalvo, F. J.; Frechet, J. M.; Thompson, P. M. *Science* **1995**, *268*, 1463.

(2) El-Shall, M. S.; Slack, W. *Macromolecules* **1995**, *28*, 8456.

(3) Collins, D. E.; Slamovich, E. B. *Chem. Mater.* **1999**, *11*, 2319.

(4) von Werne, T.; Patten, T. E. *J. Am. Chem. Soc.* **2001**, *123*, 7497.

(5) Breimer, M. A.; Yevgeny, G.; Sy, S.; Sadik, O. A. *Nano Lett.* **2001**, *1*, 305.

(6) Lin, Y.; Boeker, A.; He, J.; Sill, K.; Xiang, H.; Abetz, C.; Li, X.; Wang, J.; Emrick, T.; Long, S.; Wang, Q.; Balazs, A.; Russell, T. P. *Nature* **2005**, *434*, 55.

(7) Murphy, C. J.; Orendorff, C. J. *Adv. Mater.* **2005**, *17*, 2173.

(8) Cui, T.; Cui, F.; Zhang, J.; Wang, J.; Huang, J.; Lue, C.; Chen, Z.; Yang, B. *J. Am. Chem. Soc.* **2006**, *128*, 6298.

(9) Xiong, H.-M.; Wang, Z.-D.; Xia, Y.-Y. *Adv. Mater.* **2006**, *18*, 748.

(10) El-Shall, M. S.; Bahta, A.; Rabeony, H. M.; Reiss, H. *J. Chem. Phys.* **1987**, *87*, 1329.

(11) Reiss, H. *Science* **1987**, *238*, 1368.

(12) Reiss, H. *Acc. Chem. Res.* **1997**, *30*, 297.

(13) El-Shall, M. S.; Reiss, H. *J. Phys. Chem.* **1988**, *92*, 1021.

(14) El-Shall, M. S.; Abdelsayed, V.; Pithawalla, Y. B.; Alsharach, E.; Deevi, S. C. *J. Phys. Chem. B* **2003**, *107*, 2882.

(15) Alsharaeh, E. H.; Ibrahim, Y. M.; El-Shall, M. S. *J. Am. Chem. Soc.* **2005**, *127*, 6164.

(16) von Helden, G.; Wyttenbach, T.; Bowers, M. T. *Science* **1995**, *267*, 1483.

(17) Jarrold, M. F. *Annu. Rev. Phys. Chem.* **2000**, *51*, 179.

(18) Rusyniak, M. J.; Ibrahim, Y. M.; Wright, D. L.; Khanna, S. N.; El-Shall, M. S. *J. Am. Chem. Soc.* **2003**, *125*, 12001.

(19) Mesleh, M. F.; Hunter, J. M.; Shvartsburg, A. A.; Schatz, G. C.; Jarrold, M. F. *J. Phys. Chem.* **1996**, *100*, 16082.

(20) Frisch, M. J.; Trucks, G. W.; Schlegel, H. B.; Scuseria, G. E.; Robb, M. A.; Cheeseman, J. R.; Zakrzewski, V. G.; Montgomery, J. A., Jr.; Stratmann, R. E.; Burant, J. C.; Dapprich, S.; Millam, J. M.; Daniels, A. D.; Kudin, K. N.; Strain, M. C.; Farkas, O.; Tomasi, J.; Barone, V.; Cossi, M.; Cammi, R.; Mennucci, B.; Pomelli, C.; Adamo, C.; Clifford, S.; Ochterski, J.; Petersson, G. A.; Ayala, P. Y.; Cui, Q.; Morokuma, K.; Malick, D. K.; Rabuck, A. D.; Raghavachari, K.; Foresman, J. B.; Cioslowski, J.; Ortiz, J. V.; Stefanov, B. B.; Liu, G.; Liashenko, A.; Piskorz, P.; Komaromi, I.; Gomperts, R.; Martin, R. L.; Fox, D. J.; Keith, T.; Al-Laham, M. A.; Peng, C. Y.; Nanayakkara, A.; Gonzalez, C.; Challacombe, M.; Gill, P. M. W.; Johnson, B. G.; Chen, W.; Wong, M. W.; Andres, J. L.; Head-Gordon, M.; Replogle, E. S.; Pople, J. A. *Gaussian 98*, revision A.11.3; Gaussian, Inc.: Pittsburgh, PA, 2002.

(21) Khuong, K. S.; Jones, W. H.; Pryor, W. A.; Houk, K. N. *J. Am. Chem. Soc.* **2005**, *127*, 1265.